



## Synthesis and NLO behavior of Oligo(phenylenevinylene)-Porphyrin Dendrimers

Guadalupe G. Flores-Rojas<sup>a</sup>, Irina V. Lijanov<sup>b</sup>, Omar G. Morales-Saavedra<sup>c</sup>, Karla Sanchez-Montes<sup>a</sup>, Marcos Martínez-García<sup>a,\*</sup>

<sup>a</sup>Instituto de Química, Universidad Nacional Autónoma de México, Cd. Universitaria, Circuito Exterior, Coyoacán, México D.F. C.P. 04510, Mexico

<sup>b</sup>Instituto Politécnico Nacional, CIITEC, Cerrada Cecati S/N, Colonia Santa Catarina de Azcapotzalco, México D.F. C.P. 02250, Mexico

<sup>c</sup>Centro de Ciencias Aplicadas y Desarrollo Tecnológico, Universidad Nacional Autónoma de México, CCADET-UNAM, Circuito exterior S/N, Ciudad Universitaria, México D.F. C.P. 04510, Mexico

### ARTICLE INFO

#### Article history:

Received 28 May 2012

Received in revised form

16 July 2012

Accepted 17 July 2012

Available online 31 July 2012

#### Keywords:

Porphyrin

$\pi$ -Conjugated dendrons;

Dendrimers

OPV

Linear optics

Non-linear optics

### ABSTRACT

Dendrons with a porphyrin core and  $\pi$ -conjugated dendron branches with 8 and 16 stilbene groups have been synthesized and characterized. The dendrons used for dendrimer synthesis possessed an all *trans* configuration. Cubic non-linear optical behavior of the styryl and porphyrin-containing dendrimers was tested via Z-Scan measurements in spin-coated film samples.

© 2012 Elsevier Ltd. All rights reserved.

## 1. Introduction

In the past decades, the design and synthesis of  $\pi$ -conjugated dendrimers has been explored extensively as active chemical components in a wide range of electronic and optoelectronic devices [1].  $\pi$ -Conjugated dendrimers with electron-donating units, such as thiophene [2], carbazole [3], and phenothiazine [4], have attracted much attention because of their excellent electroluminescent and electroconductive properties, and because their size and architecture can be specifically controlled during synthesis [5]: the globular shape of dendrimers provides a large surface area that can be decorated with different chromophore species, thus resulting in a large absorption cross-section and enabling efficient capture of photons [6]. The nonlinear optical (NLO) properties of several dendrimers have been published [7–15]. Recently, we reported on dendrimers containing oligo(phenylenevinylene) branches or ferrocenyl end groups with a resorcinarene or porphyrin core with interesting optical properties [13]. Here, we report the synthesis and cubic NLO behavior of first and second generation dendrimers with  $\pi$ -conjugated branches and a porphyrin core.

## 2. Experimental

### 2.1. Reagents and instrumentation

Solvents and reagents were purchased as reagent grade and used without further purification. Acetone was distilled over calcium chloride. Tetrahydrofuran was distilled from sodium and benzophenone. Column chromatography was performed on Merck silica gel 60Å (70–230 mesh). <sup>1</sup>H- and <sup>13</sup>C-NMR were recorded on a Varian-Unity-300 MHz with tetramethylsilane (TMS) as an internal reference. Infrared (IR) spectra were measured on a spectrophotometer Nicolet FT-SSX. Elemental analysis was determined by Galbraith Laboratories Inc. (Knoxville, TN, USA). FAB+ mass spectra were taken on a JEOL JMS AX505 HA instrument. Electrospray mass spectra were taken on a Bruker Daltonic, Esquire 6000. MALDI-TOF mass spectra were taken on a Bruker Omni FLEX.

### 2.2. Synthesis of substituted benzaldehydes

A mixture of **1** or **6** (38 mmol), **2** (18.9 mmol), Pd(OAc)<sub>2</sub> (1.3 mmol), and tri-*o*-tolylphosphine TOP (3.28 mmol) in Et<sub>3</sub>N/DMF 1:5 (120 mL) was stirred under N<sub>2</sub> at 120 °C for 24 h. After cooling, the resulting mixture was filtered and the solvents evaporated. The

\* Corresponding author.

E-mail address: [margar@servidor.unam.mx](mailto:margar@servidor.unam.mx) (M. Martínez-García).

crude product was purified by column chromatography (SiO<sub>2</sub>, hexane).

### 2.2.1. (*E*) 3,5-distyrylbenzaldehyde **3**

Yield 3.5 g, (60%), white powder, m.p. 125–127 °C, UV CH<sub>2</sub>Cl<sub>2</sub> (nm): 242, 311. IR (KBr, cm<sup>-1</sup>): 3443, 3025, 2809, 2738, 1695 (C=O), 1590, 1449, 1143, 966, 884, 743, 694, 528. <sup>1</sup>H NMR (300 MHz, CDCl<sub>3</sub>), δ<sub>H</sub> (ppm): 7.13 (d, 2H, CH=, *J* = 16.5 Hz), 7.23 (d, 2H, CH=, *J* = 16.5 Hz), 7.27–7.45 (m, 4H, Ar), 7.35 (t, 2H, Ar, *J* = 1.6 Hz), 7.54–7.60 (m, 4H, Ar), 7.87 (t, 2H, Ar, *J* = 2.0 Hz), 7.92 (s, 1H, Ar), 10.09 (s, 1H, HC=O). <sup>13</sup>C NMR (75 MHz, CDCl<sub>3</sub>), δ<sub>C</sub> (ppm): 126.2 (CH=), 126.7 (Ar), 127.0 (CH=), 128.2 (Ar), 128.8 (Ar), 130.2 (Ar), 130.7 (Ar), 136.6 (Ar<sub>ipso</sub>), 137.2 (Ar<sub>ipso</sub>), 138.7 (Ar), 192.2 (C=O). MS, EI+ (*m/z*): 310. Anal. calcd. for C<sub>23</sub>H<sub>18</sub>O: C 89.00, H 5.85%. Found: C 89.10, H 5.86%

### 2.2.2. 3,5-Bis((*E*)-3,5-di(*E*)-styrylstyryl)benzaldehyde **7**

Yield 9.5 g, (70%), white powder, m.p. 131–133 °C, UV CHCl<sub>3</sub> (nm): 242.5, 316.5. IR (KBr, cm<sup>-1</sup>): 3653, 3380, 3078, 3055, 3025, 2958, 2924, 2852, 2730, 1943, 1876, 1798, 1695 (C=O), 1635, 1591, 1493, 1450, 1383, 1280, 1178, 1137, 1080, 1029, 959, 876, 831, 805, 749, 719, 691, 567, 533, 491; <sup>1</sup>H NMR (300 MHz, CDCl<sub>3</sub>), δ<sub>H</sub> (ppm): 7.17 (d, 8H, CH=, *J* = 16.2 Hz), 7.24 (d, 4H, CH=, *J* = 16.5 Hz), 7.29–7.32 (m, 4H, Ar), 7.37–7.42 (m, 8H, Ar), 7.56–7.61 (m, 8H, Ar), 7.95 (t, 2H, Ar, *J* = 1.5 Hz), 7.97 (s, 6H, Ar), 7.98 (s, 1H, Ar), 10.11 (s, 1H, HC=O). <sup>13</sup>C NMR (75 MHz, CDCl<sub>3</sub>), δ<sub>C</sub> (ppm): 124.0 (Ar), 124.5 (Ar), 126.6 (CH=), 127.5 (Ar), 127.8 (Ar), 128.1 (Ar), 128.7 (Ar), 129.5 (Ar), 130.2 (Ar), 130.4 (Ar), 137.1 (Ar<sub>ipso</sub>), 137.4 (Ar<sub>ipso</sub>), 138.2 (Ar<sub>ipso</sub>), 138.6 (Ar<sub>ipso</sub>), 192.1 (C=O). MS, FAB+ (*m/z*): 718. Anal. calcd. for C<sub>55</sub>H<sub>42</sub>O: C 91.99, H 5.89%. Found: C 91.97, H 5.76%

## 2.3. Reduction of substituted benzaldehydes

Lithium aluminum hydride (97%, 15.2 mmol) was dissolved in dry THF (50 mL). To this solution, **3** or **7** (6.4 mmol) dissolved in dry THF 15 mL were added dropwise using an addition funnel. The reaction was carried out at 0 °C for 4 h. After this time, water (10 mL) was cautiously added and the reaction mixture was filtered in Celite®. The solvent was evaporated and the residue was dissolved in dichloromethane. The resulting solution was dried with sodium sulfate, filtered and the product was vacuum dried, and purified by column chromatography (Al<sub>2</sub>O<sub>3</sub>, hexane).

### 2.3.1. (*E*)-3,5-(Distyrylphenyl) methanol **4**

Yield 1.8 g (90%), white powder, m.p. 123–125 °C, UV CH<sub>2</sub>Cl<sub>2</sub> (nm): 241, 302. IR (KBr, cm<sup>-1</sup>): 3370, 3025, 2883, 1595, 1493, 1449, 1029, 961, 750, 693. <sup>1</sup>H NMR (300 MHz, CDCl<sub>3</sub>), δ<sub>H</sub> (ppm): 4.75 (s, 2H, CH<sub>2</sub>), 5.18 (s, 1H, OH), 7.15 (s, 2H, CH=), 7.16 (s, 2H, CH=), 7.23–7.44 (m, 10H, Ar), 7.51 (d, 2H, Ar, *J* = 1.5 Hz), 7.55 (t, 1H, Ar, *J* = 1.5 Hz). <sup>13</sup>C NMR (75 MHz, CDCl<sub>3</sub>), δ<sub>C</sub> (ppm): 65.2 (CH<sub>2</sub>-OH), 124.0 (Ar), 124.2 (Ar), 126.5 (Ar), 127.7 (CH=), 128.1 (CH=), 128.7 (Ar), 129.2 (Ar), 137.1 (Ar<sub>ipso</sub>), 138.0 (Ar<sub>ipso</sub>), 141.6 (Ar). MS, EI+ (*m/z*): 312. Anal. calcd. for C<sub>23</sub>H<sub>20</sub>O: C 88.46, H 6.41%. Found: C 88.49, H 6.38%.

### 2.3.2. (3,5-bis((*E*)-3,5-di(*E*)-styrylstyryl)phenyl)methanol **8**

Yield 4.1 g (90%), white powder, m.p. 148–150 °C, UV CH<sub>2</sub>Cl<sub>2</sub> (nm): 232, 315. IR (KBr, cm<sup>-1</sup>): 3386, 3054, 3025, 2956, 2925, 2866, 1632, 1591, 1492, 1448, 1378, 1336, 1301, 1242, 1208, 1157, 1067, 1028, 958, 876, 834, 748, 691, 574, 532, 491. <sup>1</sup>H NMR (300 MHz, CDCl<sub>3</sub>), δ<sub>H</sub> (ppm): 4.70 (s, 1H, OH), 4.78 (s, 2H, CH<sub>2</sub>), 7.15 (d, 4H, CH=, *J* = 16.2 Hz), 7.22 (d, 8H, CH=, *J* = 16.8 Hz), 7.26–7.31 (m, 4H, Ar), 7.36–7.41 (m, 8H, Ar), 7.49–7.55 (m, 8H, Ar), 7.56–7.59 (m, 8H, Ar), 7.64 (t, 1H, Ar, *J* = 1.5 Hz). <sup>13</sup>C NMR (75 MHz, CDCl<sub>3</sub>), δ<sub>C</sub> (ppm): 65.0 (CH<sub>2</sub>-OH), 123.9 (Ar), 124.1 (Ar), 126.5 (CH=), 127.7 (Ar), 128.3

(Ar), 128.7 (Ar), 128.9 (Ar), 129.2 (Ar), 137.2 (Ar), 137.8 (Ar<sub>ipso</sub>), 137.9 (Ar<sub>ipso</sub>), 138.0 (Ar<sub>ipso</sub>), 141.8 (Ar<sub>ipso</sub>). MS, FAB+ (*m/z*): 720. Anal. calcd. for C<sub>55</sub>H<sub>44</sub>O: C 91.63, H 6.15%. Found: C 91.47, H 6.18%.

## 2.4. Preparation of chloromethylbenzenes

Compound **4** or **8** (14.0 mmol), pyridine (1 mL, 14.0 mmol) and SOCl<sub>2</sub> (1.45 mL, 14.0 mmol) were dissolved in dry CH<sub>2</sub>Cl<sub>2</sub> (100 mL) then, this mixture was cooled to –10 °C. The reaction was carried out under nitrogen atmosphere in ice bath for 7 h. After this period, the solvent was evaporated and the resulting oil was dry supported and purified in a silica gel (60–240 pore size) column using a mixture of hexane-dichloromethane 2:1 as eluent.

### 2.4.1. (*E*)-1-(Chloromethyl)-3,5-distyrylbenzene **5**

Yield 4.1 g (90%), yellow-brown powder, m.p. 106–108 °C, UV CHCl<sub>3</sub> (nm): 242, 302. IR (KBr, cm<sup>-1</sup>): 3026, 2924, 2953, 1596, 1493, 1450, 1261, 1155, 960, 750, 691. <sup>1</sup>H NMR (300 MHz, CDCl<sub>3</sub>), δ<sub>H</sub> (ppm): 4.63 (s, 2H, CH<sub>2</sub>-Cl), 7.13 (d, 2H, CH=, *J* = 16.4 Hz), 7.15 (d, 2H, CH=, *J* = 16.6 Hz), 7.23–7.52 (m, 10H, Ar), 7.55 (t, 2H, Ar, *J* = 2.5 Hz), 7.58 (t, 1H, Ar, *J* = 1.5 Hz). <sup>13</sup>C NMR (75 MHz, CDCl<sub>3</sub>), δ<sub>C</sub> (ppm): 46.1 (CH<sub>2</sub>-Cl), 124.7 (Ar), 125.6 (Ar), 126.5 (Ar), 127.8 (CH=), 129.6 (Ar), 136.9 (Ar<sub>ipso</sub>), 138.1 (Ar<sub>ipso</sub>), 138.2 (Ar). MS, EI+ (*m/z*): 330. Anal. calcd. for C<sub>23</sub>H<sub>19</sub>Cl: C 83.50, H 5.79%. Found: C 83.56, H 5.78%.

### 2.4.2. 5,5'-(1*E*,1'*E*)-2,2'-(5-(Chloromethyl)-1,3-phenylene) bis(ethene-2,1-diyl)bis(1,3-di(*E*)-styrylbenzene) **9**

Yield 9.3 g (90%), yellow-brown powder, m.p. 156–158 °C, UV CHCl<sub>3</sub> (nm): 232, 316. IR (KBr, cm<sup>-1</sup>): 3413, 3056, 3025, 2957, 2869, 1634, 1592, 1538, 1489, 1449, 1331, 1255, 1204, 1160, 1071, 958, 881, 834, 749, 690, 608, 564, 533, 491, 440. <sup>1</sup>H NMR (300 MHz, CDCl<sub>3</sub>), δ<sub>H</sub> (ppm): 4.66 (s, 2H, CH<sub>2</sub>), 7.15 (d, 4H, CH=, *J* = 16.4 Hz), 7.23 (d, 8H, CH=, *J* = 16.2 Hz), 7.29 (s, 4H, Ar), 7.31–7.50 (m, 16 H, Ar), 7.55–7.58 (m, 8H, Ar), 7.68 (br, 1H, Ar). <sup>13</sup>C NMR (75 MHz, CDCl<sub>3</sub>), δ<sub>C</sub> (ppm): 46.3 (CH<sub>2</sub>), 123.9 (Ar), 124.3 (Ar), 124.8 (Ar), 125.9 (Ar), 126.5 (CH=), 127.2 (Ar), 127.8 (Ar), 128.2 (Ar), 128.4 (Ar), 128.7 (Ar), 129.4 (Ar), 137.1 (Ar), 137.7 (Ar), 138.1 (Ar), 138.3 (Ar<sub>ipso</sub>), 138.5 (Ar<sub>ipso</sub>), 141.3 (Ar<sub>ipso</sub>), 145.6 (Ar<sub>ipso</sub>). MS, FAB+ (*m/z*): 738. Anal. calcd. for C<sub>55</sub>H<sub>43</sub>Cl: C 89.34, H 5.86, Cl 4.79%. Found: C 89.32, H 5.76%.

## 2.5. Preparation of vinylbenzene **6**

Compound **3** (16.1 mmol) dissolved in dry THF (10 mL) was added to a mixture of methyl triphenylphosphine (16.1 mmol) in dry THF (100 mL) and *n*-butyl lithium 2.5 M in hexanes (16.1 mmol) at 0 °C in N<sub>2</sub> atmosphere. The mixture was stirred for 24 h, then water was added (300 mL). The organic phase was evaporated to dryness and purified by column chromatography using hexane: ethyl acetate 4:1. Yield 4.6 g (92%), yellow-brown powder, m.p. 108–110 °C, UV CHCl<sub>3</sub> (nm): 312. IR (KBr, cm<sup>-1</sup>): 3080, 3027, 2979, 2959, 2924, 2853, 1954, 1880, 1804, 1665, 1628, 1590, 1492, 1449, 1407, 1384, 1329, 1301, 1264, 1241, 1178, 1156, 1072, 1053, 1025, 984, 964, 913, 882, 835, 753, 693, 668, 585, 553, 533, 511, 484, 447. <sup>1</sup>H NMR (300 MHz, CDCl<sub>3</sub>), δ<sub>H</sub> (ppm): 5.32 (d, 1H, CH<sub>2</sub>=, *J* = 11.0 Hz), 5.84 (d, 1H, CH=, *J* = 17.6 Hz), 6.77 (q, 1H, CH=), 7.15 (s, 2H, CH=), 7.16 (s, 2H, CH=), 7.23–7.46 (m, 10H, Ar), 7.52 (q, 2H, Ar), 7.56 (t, 1H, Ar, *J* = 1.6 Hz). <sup>13</sup>C NMR (75 MHz, CDCl<sub>3</sub>), δ<sub>C</sub> (ppm): 114.5 (CH=), 123.6 (Ar), 122.1 (Ar), 126.5 (Ar), 127.7 (CH=), 128.3 (Ar), 128.7 (Ar), 129.2 (Ar), 136.6 (CH=), 137.2 (Ar<sub>ipso</sub>), 137.9 (Ar<sub>ipso</sub>), 138.2 (Ar<sub>ipso</sub>). MS, EI+ (*m/z*): 308. Anal. calcd. for C<sub>24</sub>H<sub>20</sub>O: C 93.46%, H 6.54%. Found: C 93.44, H 6.44%.

## 2.6. Synthesis procedures and characterization data of new dendrimers

A mixture of the respective dendron **5** or **9** (1 mmol), potassium carbonate (21.2 mmol), and 18-crown-6 (0.56 g, 2.12 mmol) in dry acetone (80 mL) was heated to reflux and stirred vigorously in nitrogen atmosphere for 20 min porphyrin **10** (0.125 mmol) dissolved in dry acetone (40 mL) were added dropwise and the reaction was continued for 7 days. The mixture was cooled and the precipitate was filtered. The filtrate was evaporated to dryness under reduced pressure. The residue dissolved in diethyl ether was washed with an aqueous solution of 5% Na<sub>2</sub>CO<sub>3</sub> (three times). The organic layer was dried and evaporated to dryness and the dendrimers were purified using the following procedure: the dendrimer was dissolved in CH<sub>2</sub>Cl<sub>2</sub>, then methanol was added producing precipitation of the dendrimer back. This procedure was repeated three times.

### 2.6.1. Dendrimer **11**

Yield 0.66 g (55%), purple solid, m.p. 226 °C, UV–vis CH<sub>2</sub>Cl<sub>2</sub> (nm): 231, 302, 422, 454, 518, 556, 595, 651, 694. IR (KBr, cm<sup>-1</sup>): 3434, 2056, 3026, 2922, 2857, 1655, 1636, 1600, 1500, 1453, 1406, 1379, 1284, 1235, 1174, 1111, 1068, 1015, 987, 960, 881, 839, 799, 748, 692, 664, 534, 489. <sup>1</sup>H NMR (300 MHz, CDCl<sub>3</sub>) δ<sub>H</sub> (ppm): -2.68 (s, 2H, H–N), 5.3 (s, 8H, CH<sub>2</sub>), 7.25 (s, 40H, Ar), 7.28 (d, 2H, Ar, *J* = 1.5 Hz), 7.34 (d, 8H, Ar, *J* = 9 Hz), 7.35 (s, 4H, Ar), 7.38 (d, 8H, CH=, *J* = 14.7 Hz), 7.41 (d, 8H, CH=, *J* = 14.7 Hz), 7.43 (t, 2H, Ar, *J* = 1.5 Hz), 7.58–7.61 (m, 4H, Ar), 8.11 (d, 8H, Ar, *J* = 9.0 Hz), 8.87 (s, 8H, py). <sup>13</sup>C NMR (75 MHz, CDCl<sub>3</sub>) δ<sub>C</sub> (ppm): 70.3 (CH<sub>2</sub>-O), 113.1 (Ar), 119.7 (Ar), 124.62 (Ar), 125.4 (Ar), 126.6 (Ar), 127.8 (CH=), 128.2 (CH=), 128.7 (Ar), 129.6 (Ar), 135.0 (Ar<sub>ipso</sub>), 135.6 (Ar<sub>ipso</sub>), 137.2 (Ar<sub>ipso</sub>), 137.9 (Ar<sub>ipso</sub>), 138.2 (Ar<sub>ipso</sub>), 158.6 (Ar<sub>ipso</sub>). ESI MS (*m/z*): 1856. Anal. Calcd. for C<sub>136</sub>H<sub>102</sub>N<sub>4</sub>O<sub>4</sub>: C, 88.09, H, 5.53, N, 2.95%. Found: C, 88.06, H, 5.55%.

### 2.6.2. Dendrimer **12**

Yield 0.237 g (52%), purple solid, m.p. 294 °C, UV–vis CH<sub>2</sub>Cl<sub>2</sub> (nm): 231, 302, 422, 454, 518, 556, 595, 651, 694. IR (KBr, cm<sup>-1</sup>): 3434, 2056, 3026, 2922, 2857, 1655, 1636, 1600, 1500, 1453, 1406, 1379, 1284, 1235, 1174, 1111, 1068, 1015, 987, 960, 881, 839, 799, 748, 692, 664, 534, 489. <sup>1</sup>H NMR (300 MHz, CDCl<sub>3</sub>) δ<sub>H</sub> (ppm): -2.68 (s, 2H, H–N), 5.32 (s, 8H, CH<sub>2</sub>), 7.26 (s, 80H, Ar), 7.29 (t, 6H, Ar, *J* = 1.5 Hz), 7.36 (d, 8H, Ar, *J* = 9 Hz), 7.39 (d, 24H, CH=, *J* = 14.7 Hz), 7.43 (d, 24H, CH=, *J* = 14.7 Hz), 7.45 (t, 6H, Ar, *J* = 1.5 Hz), 7.58–7.61 (m, 24H, Ar), 8.12 (d, 8H, Ar, *J* = 9.0 Hz), 8.88 (s, 8H, py). <sup>13</sup>C NMR

(75 MHz, CDCl<sub>3</sub>) δ<sub>C</sub> (ppm): 71.3 (CH<sub>2</sub>-O), 113.2 (Ar), 119.7 (Ar), 124.4 (Ar), 125.4 (Ar), 126.1 (Ar), 127.8 (CH=), 128.3 (CH=), 128.7 (Ar), 129.6 (Ar), 135.1 (Ar<sub>ipso</sub>), 134.9 (Ar<sub>ipso</sub>), 136.9 (Ar<sub>ipso</sub>), 137.5 (Ar<sub>ipso</sub>), 138.2 (Ar<sub>ipso</sub>), 158.9 (Ar<sub>ipso</sub>). ESI MS (*m/z*): 3510. Anal. Calcd for C<sub>264</sub>H<sub>198</sub>N<sub>4</sub>NaO<sub>4</sub>: C, 90.25, H, 5.68, N, 1.59%. Found: C, 90.22, H, 5.64%.

## 3. Results and discussion

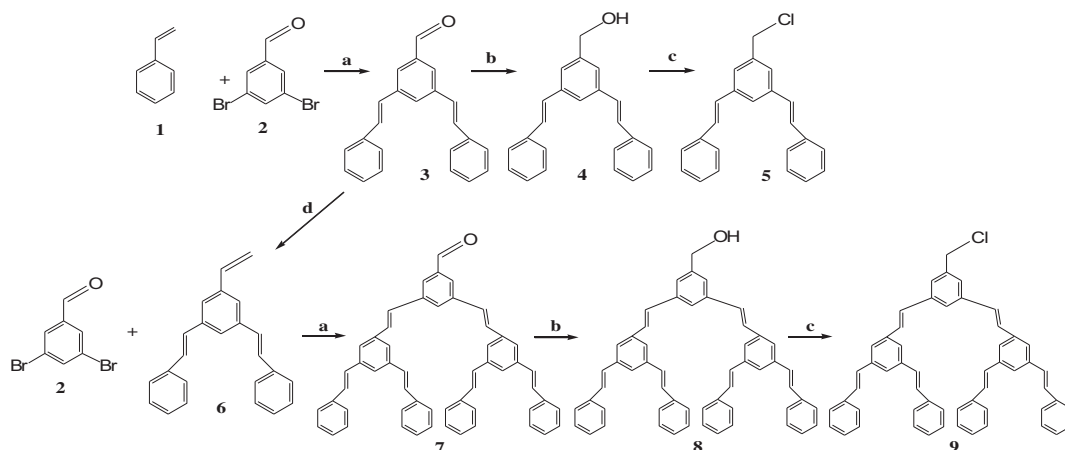
The synthesis of the two series of dendrimers with vinyl stilbene was carried out applying the convergent Fréchet approach [16]. Dendrons of first and second generations containing styryl groups were prepared using the Heck reaction in agreement with the literature data [14]. Dendrons **5** and **9** are the first and second-generation dendrons of the stilbene families (Scheme 1).

The synthesis of functionalized dendrimers **11** and **12** involves *O*-alkylation of dendrons **5** or **9** with porphyrin **10** (Scheme 2). The reaction was carried out in acetone and K<sub>2</sub>CO<sub>3</sub> at reflux for 7 days. The dendrimers **11** and **12** were dissolved in CH<sub>2</sub>Cl<sub>2</sub> and precipitated with methanol, obtaining 55 and 52% yields respectively. No side products were observed for <sup>1</sup>H, <sup>13</sup>C NMR and mass spectrometry.

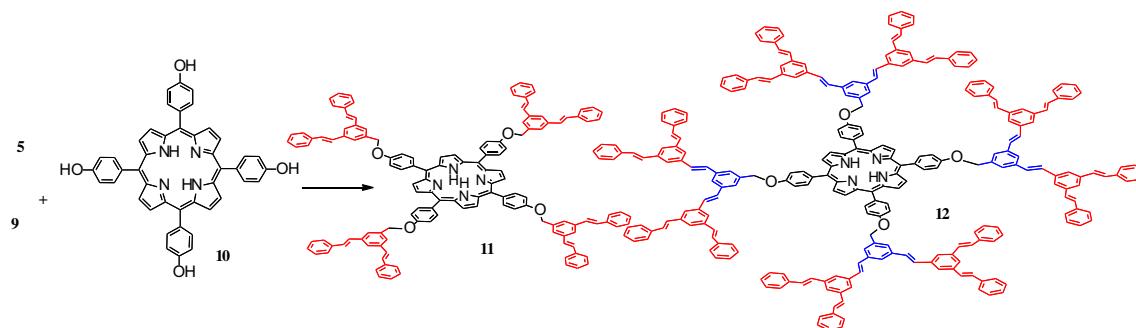
The <sup>1</sup>H NMR spectra of dendrimers **11** and **12** showed one broad signal at δ<sub>H</sub>-2.68 due the protons inside the porphyrin ring, a broad signal at δ<sub>H</sub> 5.3, and 5.32 due to the –CH<sub>2</sub>–O protons. The vinylic protons gave two doublets, at δ<sub>H</sub> 7.38 and 7.41 both showed *trans* configuration with a couplet constant *J* = 14.7 Hz. In both cases a broad peak is also observed at δ<sub>H</sub> 7.25–7.43 assigned to the aromatic protons. Finally, one singlet was observed at δ<sub>H</sub> 8.87 due to the protons at the pyrrole ring.

## 4. Linear and third order nonlinear optical properties

Regarding the linear and nonlinear optical properties of the obtained OPV-porphyrin dendrimers, homogeneous film samples were spin-coated onto glass substrates (at ~0.33 g L<sup>-1</sup> concentration, Mw: 1854.76 g mol<sup>-1</sup> and 3487.54 g mol<sup>-1</sup> for compounds **11** and **12**, respectively), with average film thickness of ~100 nm and highest optical and film deposition quality were selected for cubic NLO-characterization via the Z-Scan technique. Fig. 1a shows the optical spectra (absorption coefficients) recorded within the visible range for the studied films. The obtained thin films are suitable for adequate optical data analysis due to their appropriate transparency at optical wavelengths, which represents an important improvement in the NLO-efficiency/transparency trade-off



**Scheme 1.** Synthesis of dendrons of first and second generations, a) Pd(OAc)<sub>2</sub>, TOP DMF/ET<sub>3</sub>N, 120 °C; b) THF, LiAlH<sub>4</sub>, 0 °C; c) Py, CH<sub>2</sub>Cl<sub>2</sub>, SOCl<sub>2</sub>, 0 °C; d) CH<sub>3</sub>(Ph)<sub>3</sub>PBr, *n*-BuLi, THF, 0 °C.



Scheme 2. Synthesis of OPV-porphyrin dendrimers.

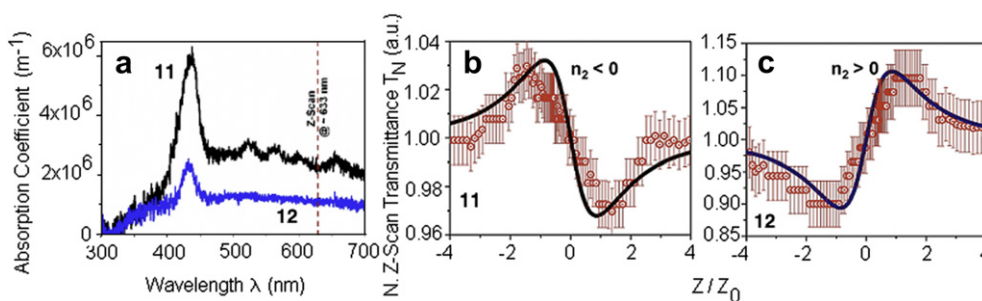


Fig. 1. a-c) Linear and Z-Scan nonlinear optical measurements (at  $\lambda_{Z\text{-Scan}} = 632.8$  nm) for compounds **11** and **12**: Linear absorption coefficients of the dendrimers **11** and **12** (a). Closed aperture Z-Scan data obtained for **11** (b), and **12** (c), based film under similar experimental conditions. An estimated experimental error below 6% is also considered for Z-Scan data (error bars). Theoretical fitting (TFs): continuous lines.

always present for organic compounds. This fact shows evidence of the importance of these materials as potential candidates for photonic and opto-electronic applications. In Fig. 1a, the optical absorbance occurs within the 400–600 nm spectral range for both dendrimer compounds indicating additional conjugation of delocalized  $\pi$ -electrons and multi-directional charge transfer properties, provided by the higher content of dendrons within the dendrimer-based film samples. This suggestion will be explored by means of NLO Z-Scan experiments as explained below. Under this framework, the available laser excitation line for Z-Scan experiments (@  $\lambda_{Z\text{-Scan}} = 632.8$  nm) is also depicted in this figure (vertical dashed line). At this wavelength, lower absorptive conditions occur, allowing non-resonant NLO-characterizations for these samples and, therefore, avoiding fast photo-degradation, thermal and self-absorptive effects during long Z-Scan measurements as much as possible (see the estimated absorption coefficients  $\alpha_0$  in Table 1). The  $\alpha_0$  values are very useful for the determination of the nonlinear refractive coefficients according to the Z-Scan technique. The film thicknesses and the estimated linear refractive indices of the studied samples are also shown in Table 1. It is worth noting that the absorption coefficient of the **11**-based film is much larger than that obtained for the **12**-based film (with similar film thickness), which is understandable given that the molecular weight (Mw) of compound **11** is, proportionally, smaller and the film

samples were prepared from similar starting solutions at  $\sim 0.33$  g L<sup>-1</sup> concentration. Indeed, the larger amount of molecules within the **11**-based film allows stronger absorptive conditions.

NLO/Z-Scan measurements were performed at room temperature on the deposited OPV porphyrin dendrimer films. The observed non-local effect of these samples is shown in Fig. 1(b,c). Theoretical fitting was performed to the experimental data in order to evaluate the nonlinear refractive properties of these compounds. The NLO-response of the deposited films was characterized by varying the polarization input planes of the He–Ne laser system in order to explore microscopic material asymmetries or anisotropies throughout the sample structure. In general, since all NLO-measurements were systematically performed with different laser input polarization states (from 0 to 90°: S- to P-polarization states, respectively) and the obtained curves are quite similar in each sample, the film structures do not seem to show any significant anisotropic behaviour, thus confirming their amorphous nature (measurements were performed in different sample points). As shown in Fig. 1(b,c), the Z-Scan experimental data obtained from compounds **11** and **12** exhibit typical peak-to-valley/valley-to-peak Z-Scan transmittance curves. Taking into account the theory developed by Sheik-Bahae et al. [17–20]. It can be observed from our measurements that the nonlinear refractive response of these samples can be unambiguously determined from these highly

Table 1  
Linear and nonlinear optical coefficients of the compounds 11 and 12 based films measured according to the Z-Scan technique. (Closed aperture Z-Scan measurements @  $\lambda_{Z\text{-Scan}} = 632.8$  nm,  $S \approx 23\%$ , Rayleigh range:  $z_0 = 3.1$  mm).

OPV-Dendrimer Film Sample	Linear Refractive Index: $n_0$ (@ 632.8 nm)	Linear Absorption Coefficient: $\alpha_0$ (@ 632.8 nm) [m <sup>-1</sup> ]	Film Thickness [nm]	NLO-Refractive Index: $\gamma/n_2$ Z-Scan @ $\lambda = 632.8$ nm $\times 10^{-8}$ [m <sup>2</sup> W <sup>-1</sup> ]/ $\times 10^{-1}$ [esu]
Compound 11	1.70 ± 0.05	2,307,841	90	-1.8/-0.7
Compound 12	1.74 ± 0.05	1,050,898	115	+42.6/+1.6

symmetrical Z-Scan transmittance curves. Hence, it can immediately be concluded that compound **11** exhibits a negative NLO-refractive coefficient ( $\gamma$  or  $n_2 < 0$ ), whereas compound **12** exhibits a substantial and positive NLO-coefficient ( $\gamma$  or  $n_2 > 0$ ).

The respective theoretical fits (TFs) to the obtained Z-Scan transmission data (solid lines) are also shown in Fig. 1(b,c). According to Table 1, the TFs allowed us to evaluate a negative NLO-refractive coefficient in the order of  $\gamma = -1.8 \times 10^{-8} \text{ m}^2 \text{ W}^{-1}$  (or  $n_2 = -0.7 \times 10^{-1} \text{ esu}$ ),<sup>1,2</sup> for the **11**-based film sample. In contrast, a positive and much larger (in magnitude) NLO-refractive coefficient was obtained for compound **12**:  $\gamma = +42.6 \times 10^{-8} \text{ m}^2 \text{ W}^{-1}$  (or  $n_2 = +1.6 \times 10^{-1} \text{ esu}$ ). The obtained  $\gamma/n_2$ -values are many orders of magnitude larger than those observed for either the typical glass substrates or for the classical CS<sub>2</sub> standard reference material:  $+1.2 \times 10^{-11} \text{ esu}$  (Z-Scan @  $\lambda = 10.6 \mu\text{m}$ ) or  $6.8 \times 10^{-13} \text{ esu}$  (DFWM @  $\lambda = 532 \text{ nm}$ ) [17–22].

One of the most interesting features of our measurements is the sign reversal of the NLO-response observed from the **11**-based film to the **12** sample. Since the amorphous films comprise randomly oriented and symmetrical disk-like dendrimer compounds, this result cannot be attributed to local material anisotropies, as has been proven by means of polarization dependent Z-Scan measurements. In fact, this phenomenon is actually strongly related to the dimension of the constituting dendrimer compounds. In other words, the length of the synthesized dendron units (compounds **5** and **9**: first and second generations, respectively) implemented to build the OPV porphyrin dendrimers plays a crucial role in the NLO behavior of these molecules. Indeed, due to the improved charge transfer and electron mobility throughout the whole OPV porphyrin dendrimer molecular structures, an enhanced nonlinearity tends to occur in both dendrimer-based film samples, being this  $\gamma/n_2$  coefficient much larger (in magnitude) for the film composed of bigger **12** dendrimer compounds despite the fact that the **11**-based film contains twice as many smaller molecular units as the **12**-based film, according to their respective molecular weights. Nevertheless, in the case of shorter molecular electronic pathways (compound with a shorter excitation cross-section), free electrons are able to in-phase follow the optical field; giving rise to a characteristic NLO-response of the **11**-based film. This agrees well with the exhibition of a smaller (in magnitude) NLO refractive index (see Fig. 1b). On the other hand, however, as the dendrimer size increases (**12**-based film) and due to the complex structure of these compounds, the hyperbranched and extremely large electronic pathways exposed by the second generation dendrons (compound **9**), provokes that the free electrons follow, in an out-of-phase oscillating configuration, the excitation optical field; thus higher molecular absorption and consequently a stronger NLO refractive property with sign reversal takes place. Indeed, the sign reversal of the refractive index can be attributed to the switching between in-phase and out-of-phase oscillations of the  $\pi$ -electron density with the molecular size.

## 5. Conclusions

The larger hyperbranched molecule (compound **12**) exhibits a giant and positive NLO-refractive coefficient in the order of  $\gamma = +42.6 \times 10^{-8} \text{ m}^2 \text{ W}^{-1}$ . In contrast, compound **11** comprising of a first generation dendron (**5**) compound exhibits lower NLO-activity. The observed sign reversal of the NLO-refractive coefficients is attributed to the dendrimer size (dendron length) and to the respective in- and out-of-phase electronic oscillating

configurations. However, more investigations should be performed on these materials in order to further understand the electronic and thermal contributions to the cubic NLO-properties taking place during long Z-Scan measurements, as well as the occurrence of possible light-induced *trans/cis* isomerization processes along the hyperbranched dendrimer composed of stilbene based dendron units.

## Acknowledgements

This work was supported by DGAPA-UNAM (IN-20210-3) grant. We would also like to thank Rios O. H., Velasco L., Huerta S. E., Patiño M. M. R., Peña Gonzalez M. A., and Garcia Rios E. for technical assistance.

## References

- Grayson SM, Fréchet JM. Convergent dendrons and dendrimers: from synthesis to applications. *Chem Rev* 2001;101:3819–67.
- Harpham MR, Suzer O, Ma CQ, Bauerle P, Goodson III T. Thiophene dendrimers as entangled photon sensor materials. *J Am Chem Soc* 2009;131:973–9.
- Loiseau F, Campagna S, Hameuraine A, Dehaen W. Dendrimers made of porphyrin cores and carbazole chromophores as peripheral units. Absorption spectra, luminescence properties, and oxidation behavior. *J Am Chem Soc* 2005;127:11352–63.
- Okamoto T, Kuratsu M, Kozaki M, Hirotsu K, Ichimura A, Matsushita T, et al. Remarkable structure deformation in phenothiazine trimer radical cation. *Org Lett* 2004;6:3493–6.
- Smith DK, Diederich F. Supramolecular dendrimer chemistry: a journey through the branched architecture. *Top Curr Chem* 2000;210:183–227.
- Balzani V, Credi A, Raymo FM, Stoddart JF. Artificial molecular machines. *Angew Chem Int Ed* 2000;39:3349–91.
- Zeng F, Zimmerman SC. Dendrimers in supramolecular chemistry: from molecular recognition to self-assembly. *Chem Rev* 1997;97:1681–712.
- Tomalia DA, Majoros I. Supramolecular polymers. New York, NY: Marcel Dekkers; 2000. p. 359.
- Newkome GR, He H, Moorefield CN. Suprasuper molecules with novel properties: Metallo dendrimers. *Chem Rev* 1999;99:1689–746.
- McClenaghan ND, Passalacqua R, Loiseau F, Campagna S, Verheyde B, Hammeurlaine A, et al. Ruthenium(II) dendrimers containing carbazole-based chromophores as branches. *J Am Chem Soc* 2003;125:5356–65.
- Emrick T, Fréchet JM. Self-assembly of dendritic structures. *Curr Opin Colloid Interf Sci* 1999;4:15–23.
- Bosman AW, Janssen HM, Meijer EW. About dendrimers: structure, physical properties, and applications. *Chem Rev* 1999;99:1665–88.
- Reyes VMI, Vázquez GRA, Klimova T, Klimova E, Ortiz FL, Martínez GM. Synthesis of ferrocenyl-bearing dendrimers with a resorcinarene core. *Inorg Chem Acta* 2008;361:1597–605.
- Lijanová IV, Reyes-Valderrama MI, Maldonado JL, Ramos-Ortiz G, Klimova T, Martínez-García M. Synthesis and cubic nonlinear optical behavior of phenyl and ferrocenyl-ended resorcinarene-based dendrimers. *Tetrahedron* 2008;64:4460–7.
- Armaroli N, Accorsi G, Rio Y, Ceroni P, Vicinelli V, Welter R, et al. Electronic properties of oligophenylenevinylene and oligophenyleneethynylene arrays constructed on the upper rim of a calix[4]arene core. *New J Chem* 2004;28:1627–37.
- Hawker CJ, Fréchet JM. Preparation of polymers with controlled molecular architecture. A new convergent approach to dendritic macromolecules. *J Am Chem Soc* 1990;112:7638–47.
- Sheik-Bahae M, Said AA, Van Stryland EW. High-sensitivity, single-beam  $n_2$  measurements. *Opt Lett* 1989;14:955–7.
- Sheik-Bahae M, Said AA, Hagan DJ, Soileau MJ, Van Stryland EW. Nonlinear refraction and optical limiting in thick media. *Opt Eng* 1991;30:1228–35.
- Sheik-Bahae M, Said AA, Hui Wei T, Hagan DJ, Van Stryland EW. Sensitive measurement of optical nonlinearities using a single beam IEEE. *J Quantum Electronics* 1990;26:760–9.
- Xia T, Hagan DJ, Sheik-Bahae M, Van Stryland EW. Eclipsing Z-scan measurement of  $\lambda \div 10$  4 wave-front distortion. *Opt Lett* 1994;19:317–9.
- Cuppo FLS, Gómez SL, Figueiredo Neto AM. Behavior of the nonlinear refractive indices and birefringence in the neighborhood of first- and second-order phase transitions in lyotropic liquid crystals. *Phys Rev E* 2003;67:051711/1–051711/5.
- Cuppo FLS, Neto AMF, Gómez SL, Palffy-Muhoray P. Thermal-lens model compared with the Sheik-Bahae formalism in interpreting Z-scan experiments on lyotropic liquid crystals. *J Opt Soc Am B* 2002;19:1342–8.

<sup>1</sup> with  $[\gamma] \equiv [\text{m}^2 \text{ W}^{-1}]$ .

<sup>2</sup> NLO refractive index in electrostatic units.  $n_2(\text{esu}) = (cn_0/40\pi)\gamma$ .